International Journal of Heat and Fluid Flow 72 (2018) 73–85

Contents lists available at ScienceDirect

International Journal of Heat and Fluid Flow

journal homepage: www.elsevier.com/locate/ijhff

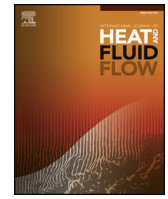

Simulations of shock wave/turbulent boundary layer interaction with upstream micro vortex generators

Arnaud Grébert*, Julien Bodart, Stéphane Jamme, Laurent Joly

Department of Aerodynamics and Propulsion (DAEP), ISAE-SUPAERO, University of Toulouse, 10 Avenue Edouard Belin, Toulouse, 31055, France

A R T I C L E I N F O

Keywords:
Shock wave
Turbulent boundary layer
Micro vortex generators
Large-eddy simulation

A B S T R A C T

The streamwise breathing motion of the separation bubble, triggered by the shock wave/boundary layer interaction (SBLI) at large Mach number, is known to yield wall pressure and aerodynamic load fluctuations. Following the experiments by Wang et al. (2012), we aim to evaluate and understand how the introduction of microramp vortex generators (mVGs) upstream the interaction may reduce the amplitude of these fluctuations. We first perform a reference large-eddy simulation (LES) of the canonical situation when the interaction occurs between the turbulent boundary layer (TBL) over a flat plate at Mach number $M = 2.7$ and Reynolds number $Re_\theta = 3600$ and an incident oblique shock wave produced on an opposite wall. A high-resolution simulation is then performed including a rake of microramps protruding by 0.47δ in the TBL. The long time integration of the simulations allows to capture 52 and 32 low-frequency oscillations for the natural case and controlled SBLI, respectively. In the natural case, we retrieve the pressure fluctuations associated with the reflected shock foot motions at low-frequency characterized by $St_L = 0.02 - 0.06$. The controlled case reveals a complex interaction between the otherwise two-dimensional separation bubble and the array of hairpin vortices shed at a much higher frequency $St_L = 2.4$ by the mVGs rake. The effect on the map of averaged wall shear stress and on the pressure load fluctuations in the interaction zone is described, with a 20% and 9% reduction of the mean separated area and pressure load fluctuations, respectively. Furthermore, the controlled SBLI exhibits a new oscillating motion of the reflected shock foot, varying in the spanwise direction with a characteristic low-frequency of $St_L = 0.1$ in the wake of the mVGs and $St_L = 0.05$ in between.

1. Introduction

Because it is ubiquitous in high Mach number internal and external flows of interest to aeronautical applications, the shock wave/turbulent boundary layer interaction (SBLI) has been the focus of many research efforts over the past decades (see the review by Clemens and Narayanaswamy, 2014). There are different flow arrangements in which the SBLI occurs, depending on the geometry and the position of the shock generator relative to the boundary layer. However, they all exhibit a large separation bubble triggered by the severe adverse pressure gradient across the shock. The massive separation gives rise to two different issues from the application standpoint. Whereas load losses at the inlet of a scramjet engine are concerned with the impact on the engine efficiency of the mean flow properties, the structural fatigue by buffet modes over transonic airfoils is due to the unsteadiness of the SBLI. We restrict ourselves to the simplest configuration that illustrates the second kind of preoccupations where an incident oblique shock wave impinges on a flat plate turbulent boundary layer (TBL).

In large upstream Mach number SBLI, the separation point and the reflected shock foot are well known to oscillate in streamwise direction at a frequency f much lower than the inverse of the characteristic travel time over the separation bubble length L_{sep}. The corresponding Strouhal number $St_L = fL_{sep}/U_\infty$ is thus small and lies in the range $0.02 - 0.06$. Though very slow, the streamwise motion of the reflected shock yields large amplitude variations of pressure signals measured at fixed positions on the wall that are alternatively located upstream and downstream the moving reflected shock foot.

No consensus about the origin of this low-frequency motion has emerged yet but two explanations are standing as good candidates and have largely benefited from recent refined simulations or upgraded experimental measurement techniques.

According to the PIV measurements carried out by Piponniau et al. (2009), the recirculating region would be drained at low frequencies in response to the KH instability of the shear layer developing along the separation line. On the other hand, Ganapathisubramani et al. (2009) report that unsteadiness is linked to

* Corresponding author.
E-mail address: arnaud.grebert@isae.fr (A. Grébert).

https://doi.org/10.1016/j.ijheatfluidflow.2018.05.001
Received 26 November 2017; Received in revised form 13 March 2018; Accepted 2 May 2018

the presence of long streamwise boundary-layer superstructures located in the lower part of the upstream boundary layer, which leads them to conclude that the low-frequency motion observed in SBLI corresponds to a selective amplification of large-scale disturbances in the incoming flow.

Besides, a great deal of effort has been directed to reduce the SBLI-induced impact on aerodynamic performances or load variations relying on classical passive control solutions, such as streamwise vortex generators, aiming at delaying or suppressing separation. Among these, vortex generators smaller than the TBL thickness, also called microramp vortex generators (mVGs), have drawn a particular attention because their induced drag remains low while they significantly enhance wall-normal momentum transfer (Lin, 2002).

In the context of SBLI Anderson et al. (2006) conducted a comprehensive evaluation by steady RANS simulations of a large number of mVGs designs to increase the recovery rate of the TBL downstream reattachment, *i.e.* to minimize the boundary layer transformed form factor H_{tr} downstream of the SBLI. Following the experimental study of Wang et al. (2012) we select the mVG rake geometry that was identified as optimal by Anderson in this respect. However, before addressing the impact of the mVGs rake on the SBLI, the flow structure downstream of the mVGs is of interest on its own (see Panaras and Lu, 2015). In Grébert et al. (2016) we confirmed that the mVG wake exhibits a highly periodic vortex shedding with counter-rotating vortex pairs forming hairpin vortices downstream.

The present large eddy simulations (LES) thus aim at clarifying the interaction between the unsteady mVGs wake and the separation bubble behind the reflected shock. We are able to compare the natural SBLI and the one impinged by the mVGs wake with respect to the frequency content of the wall-pressure fluctuations, to wall shear stress and pressure load fluctuations. We also advocate that these numerical simulations could ultimately give hints about the uncontrolled low-frequency motion mechanism.

2. Flow configuration

2.1. Large-eddy simulations set-up

This study follows our previous work and all details about the numerics and validation of the simulations can be found in Grébert et al. (2016, 2017). The present large eddy simulations were performed using the CharLES^X solver, see Bermejo-Moreno et al. (2014), which solves the spatially filtered compressible Navier–Stokes equations for conserved quantities using a finite volume formulation and a control-volume-based discretization on unstructured hexahedral meshes. An explicit third-order Runge–Kutta (RK3) scheme is used for time advancement. The solver relies on Vreman (2004) subgrid-scale (SGS) model to represent effect of unresolved small-scale fluid motions. It also features a solution-adaptive methodology which combines a non-dissipative centred numerical scheme and an essentially non-oscillatory (ENO) second-order shock-capturing scheme. The latter is applied in regions around shock waves, identified by a shock sensor sensitized (Eq. (1)) to local dilatation $\partial u_k/\partial x_k$, enstrophy $\omega_i\omega_j$, sound speed c and mesh cell size Δ (see Bermejo-Moreno et al., 2014 for more details about the numerics).

$$-\frac{\partial u_k}{\partial x_k} > \max\left(\sqrt{\omega_i\omega_j}, \frac{0.05c}{\Delta}\right) \tag{1}$$

The configuration selected in the present work follows Wang et al. (2012) experiments, as sketched in Fig. 2. It is characterized by a free stream Mach number of $M = 2.7$ and a Reynolds number $Re_\theta = 3600$ based on the turbulent boundary layer momentum thickness at the wall inviscid-impingement location of the incident shock x_{imp}. As in the experiments, a shock generator is introduced on the opposite wall with a flow deflection of $\phi = 10.5°$ yielding to an incident shock wave angle of $\beta = 33.3°$. The microramp vortex generator (mVG) geometry is

Table 1
Grid parameters for the LES with δ_0 the TBL thickness just upstream of the SBLI at $x_A^* = -1.5$.

Δx^+	Δy^+_{min}	Δz^+	L_x/δ_0	L_y/δ_0	L_z/δ_0
[7.5–20]	1	[3–15]	40	12	6

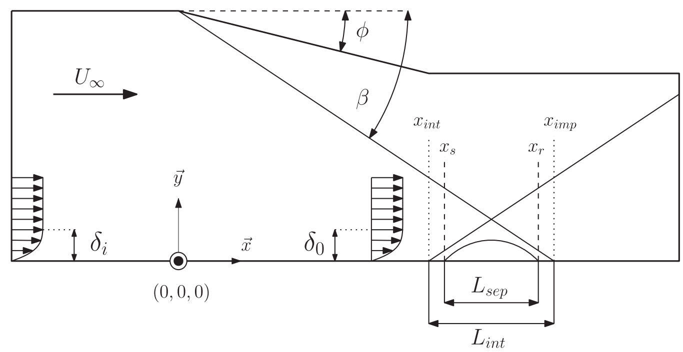

Fig. 1. Schematic of the SBLI configuration with reference parameters and length scales.

the same as in the experiments with a height of where δ_v is the TBL thickness immediately upstream of the mVG, a chord length $c = 7.2h$ and a wedge half-angle $A_p = 24°$. Two spanwise periods of the mVGs rake are introduced in the computational domain, located at $16\delta_v = 34h$ from the impingement shock incident point and at $23\delta_i$ from the inlet, δ_i being the TBL thickness at the inflow, to avoid spurious effect of the

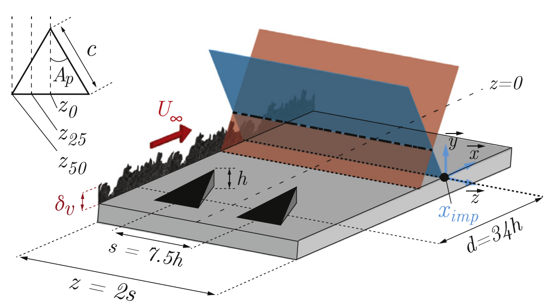

Fig. 2. Sketch and reference length scales of the configuration for the present LES with microramp vortex generators.

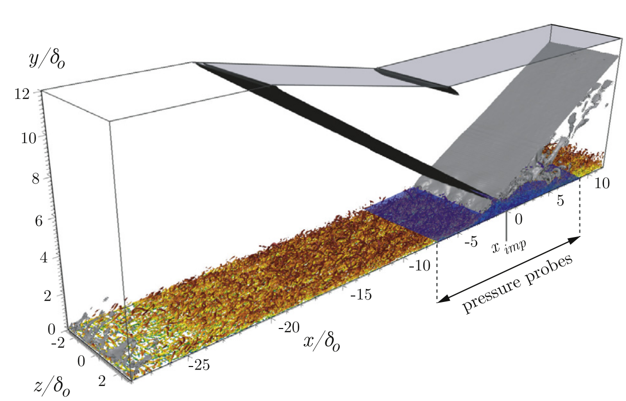

Fig. 3. Schematic view of the wall-pressure probes area (blue). (For interpretation of the references to colour in this figure legend, the reader is referred to the web version of this article.)